Quaternary International 283 (2013) 11–20

Contents lists available at SciVerse ScienceDirect

Quaternary International

journal homepage: www.elsevier.com/locate/quaint

Long-term variation of temperature over North China and its links with large-scale atmospheric circulation

Qiang Li [a], Yu Liu [a,b,*], Huiming Song [a], Qiufang Cai [a], Yinke Yang [c]

[a] State Key Laboratory of Loess and Quaternary Geology, Institute of Earth Environment, Chinese Academy of Sciences, Xi'an 710075, China
[b] School of Human Settlements and Civil Engineering, Xi'an Jiaotong University, Xi'an 710049, China
[c] Environmental Science and Engineering College, Chang'an University, Xi'an 710054, China

ARTICLE INFO

Article history:
Available online 16 March 2012

ABSTRACT

A May–July temperature reconstruction is based on tree-ring widths of Chinese pine (*Pinus tabulaeformis*) from Ningwu, Shanxi Province, China. The reconstruction explains 45.1% of the variance in observed May–July temperature. The intervals with persistent decadal warmth include 1779–1792, 1827–1839, 1853–1865, 1898–1932, 1936–1948 and 1987–2003. Intervals with persistent decadal cold include 1793–1807, 1814–1826, 1866–1888, 1949–1963 and 1976–1986. Spatial correlation between the reconstruction and the gridded temperature datasets reveals that the reconstruction is representative of temperature variability in semi-arid/arid regions of East Asia, including the Gobi Desert, the Loess Plateau and the North China Plain. The regions are referred to as North China in this study. Significant correlation with the January–August temperature reconstruction in the Helan Mountains of Northwest China for the overlapping period of 1796–1999 suggests that the reconstruction captures the regional temperature variability for a long-term period. The reconstructed temperature series has a significantly negative correlation with the monsoon rainfall series at interannual, decadal and multi-decadal time scales for the overlapping period of 1688–2003, suggesting an influence of the East Asian Summer Monsoon (EASM) and the dominant climate regime consisting of either cool/wet or warm/dry weather in the North China. Moreover, for the past three centuries, synchronous variations are found for the reconstructed temperature as well as the reconstructed Asian-Pacific Oscillation (APO) and the Pacific Decadal Oscillation (PDO) at decadal and multi-decadal time scales, suggesting the influences of large-scale atmospheric circulations on temperature variability in the North China. The possible mechanisms behind these links are also explained with observed climate data.

1. Introduction

Recent climate warming has become an issue of public concern because of its obvious impacts on society, the environment and various ecosystems. Some impacts include drying up of rivers and lakes, decreasing crop yields, frequent extreme climate events and increasing insect problems (Dillon et al., 2010; Piao et al., 2010). It is essential to understand temperature variability in a historical context to fully understand current climate warming. A historical understanding of temperature variability will clarify the relative roles of natural variability and of the anthropogenic impact on global climate. Identifying possible factors that influence temperature variability will improve ability to predict climatic change in the future, which will help to avoid disastrous environmental and ecological problems.

Reconstruction of temperatures using natural archives (e.g., tree rings, corals, ice cores and stalagmites) is essential to understanding temperature variability at the scale of the history of the Earth. In particular, tree rings, with their high resolution and reliability, play very important roles in temperature reconstructions for various terrestrial regions of the world.

East Asia is one of the world's most populated areas, home to approximately one fifth of the world's population. The climate is largely influenced by the East Asian Summer Monsoon (EASM). Strong EASM winds push the rainfall front northwestward, which brings about heavy amounts of thermal water vapor from the Pacific over East Asian countries (Lau and Li, 1984; Wang, 2001; Wang and LI, 2007). EASM is also one of the most active components of the global climate system (Wu and Wang, 2002; Ding and

* Corresponding author. State Key Laboratory of Loess and Quaternary Geology, Institute of Earth Environment, Chinese Academy of Sciences, Xi'an 710075, China.
E-mail address: liuyu@loess.llqg.ac.cn (Y. Liu).

1040-6182/$ – see front matter © 2012 Elsevier Ltd and INQUA. All rights reserved.
doi:10.1016/j.quaint.2012.03.017

Wang, 2007; Zhou et al., 2011). Because of the direct impacts of monsoonal precipitation on water resources and agriculture (Piao et al., 2010), many dendroclimatological studies have focused on precipitation (or drought) reconstructions in East Asia and these reconstructions' responses to large-scale atmospheric circulation (Hughes et al., 1994; Liu et al., 2004, 2009a, 2010; Sheppard et al., 2004; Shao et al., 2005; Garfin et al., 2005; D'Arrigo and Wilson, 2006; Li et al., 2006, 2011a; Buckley et al., 2007; Sano et al., 2009; Cook et al., 2010). However, there are few long temperature reconstructions for East Asia, which limits exploration of the relationship between temperature variability and large-scale atmospheric circulations. This study employs living Chinese Pine (*Pinus tabulaeformis*), the most widespread tree species in arid or semi-arid China, to reconstruct the temperature variations from 1676 to 2003. Then, the reconstruction is used to explore the possible links with large-scale atmospheric circulations such as EASM, APO and PDO.

2. Material and methods

2.1. Sampling site and local climate

The sampling site is located on a rocky ridge of Ningwu (NW; 38°50′N, 112°05′E; 1600–2100 m above sea level) in Shanxi Province, China (Fig. 1). This area is a typical semi-arid area. Ningwu lies in the environmentally sensitive zone of China, in a transitional area between humid and arid conditions, monsoon and non-monsoon climates, as well as forest and steppe. The temperature in this zone is extremely sensitive and could be affected positively or negatively by climate changes (Liu et al., 2010). At the sampling site, the vegetation is sparse and the soil is shallow.

According to records from the nearest meteorological station of Yuanping (38°45′N, 112°42′E; 836 m above sea level, records from 1954 to 2003), the mean annual precipitation was 428 mm during the observation period. The highest precipitation occurs in July–August,

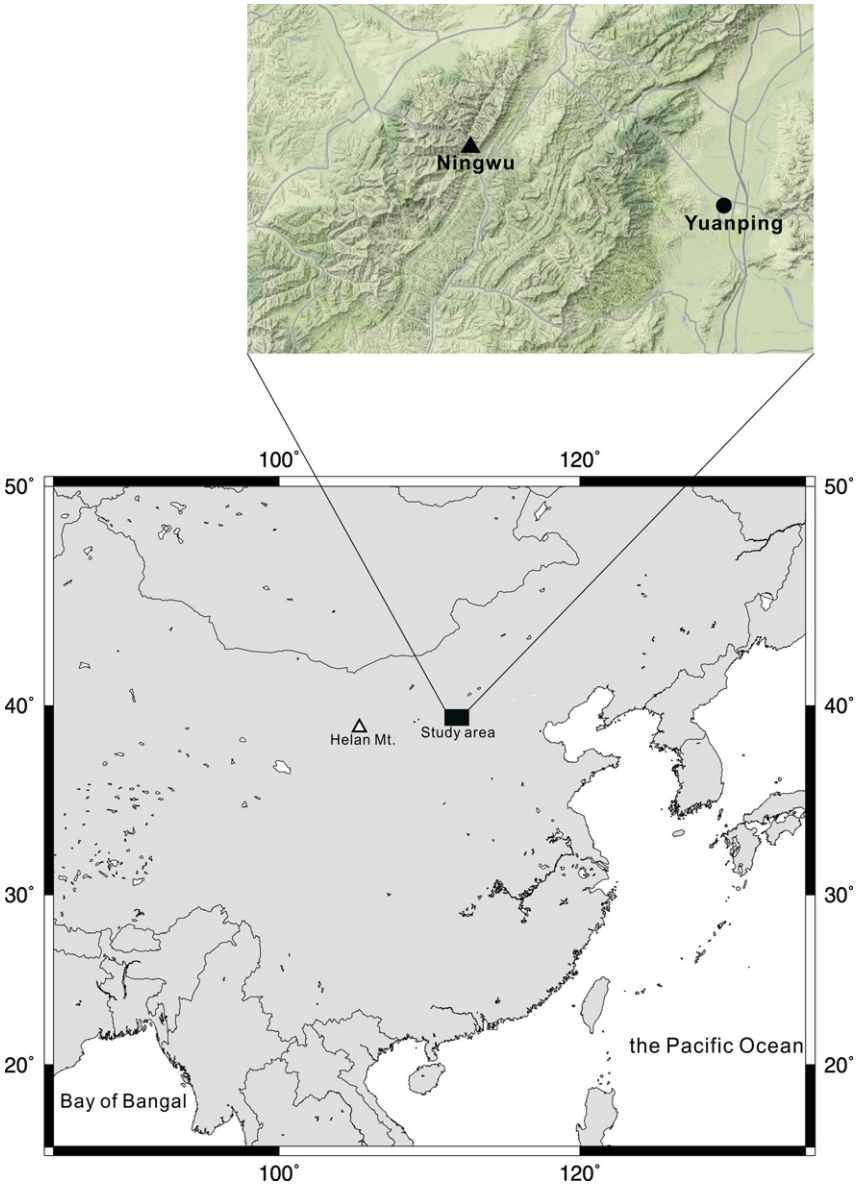

Fig. 1. Upper map showing topographic map of the study area; solid triangle and circle present the sampling site of Ningwu and Yuanping meteorological station, respectively. Lower map showing the locations of the study area and Helan Mts.

which accounts for more than half of the total annual precipitation. The mean monthly relative humidity reaches a maximum in August (73.3%). Detailed seasonal variations are shown in Fig. 2a. The inter-annual variations of mean temperature, total precipitation and relative humidity during the growing season of trees (April–September) are shown in Fig. 2b. The temperature in the study area has exhibited a rapidly increasing trend, especially since the late 1970s. Inverse trends between temperature and precipitation ($r = -0.342$, $p < 0.01$) and between temperature and relative humidity ($r = -0.548$, $p < 0.0001$) have been detected as well. Relative humidity varies synchronously with precipitation ($r = 0.708$, $p < 0.0001$).

2.2. Tree-ring samples

The dominant tree species at the sampling site is Chinese pine (*P. tabulaeformis*). The site is fairly open, with 5–10 m between trees and a discontinuous canopy. The trees sampled generally grow on thin and nutrient-poor soil or rocks at the top of the ridge. In total, 37 cores from 17 trees were sampled at breast height using 5-mm increment borers in July 2004 (Li et al., 2006, 2011b).

2.3. Development of the chronology

The tree-ring cores were surfaced, cross-dated by the Skeleton Plot method, and measured by the LINTAB of ring-width system with a precision of 0.01 mm (Stokes and Smiley, 1968). The quality control of cross-dating was carried out using the COFECHA program (Holmes, 1983). The undesirable growth trends related to age and stand dynamics but not related to climate variations were removed from each individual tree-ring series using ARSTAN software (Cook and Kairiukstis, 1990). In this step, each series was standardized using negative-exponential or straight curve fitting to preserve the maximum common signal related to climate. The mean ring-width index for the site was subsequently engendered by combining all series for each year using the bi-weight robust mean (Cook and Kairiukstis, 1990).

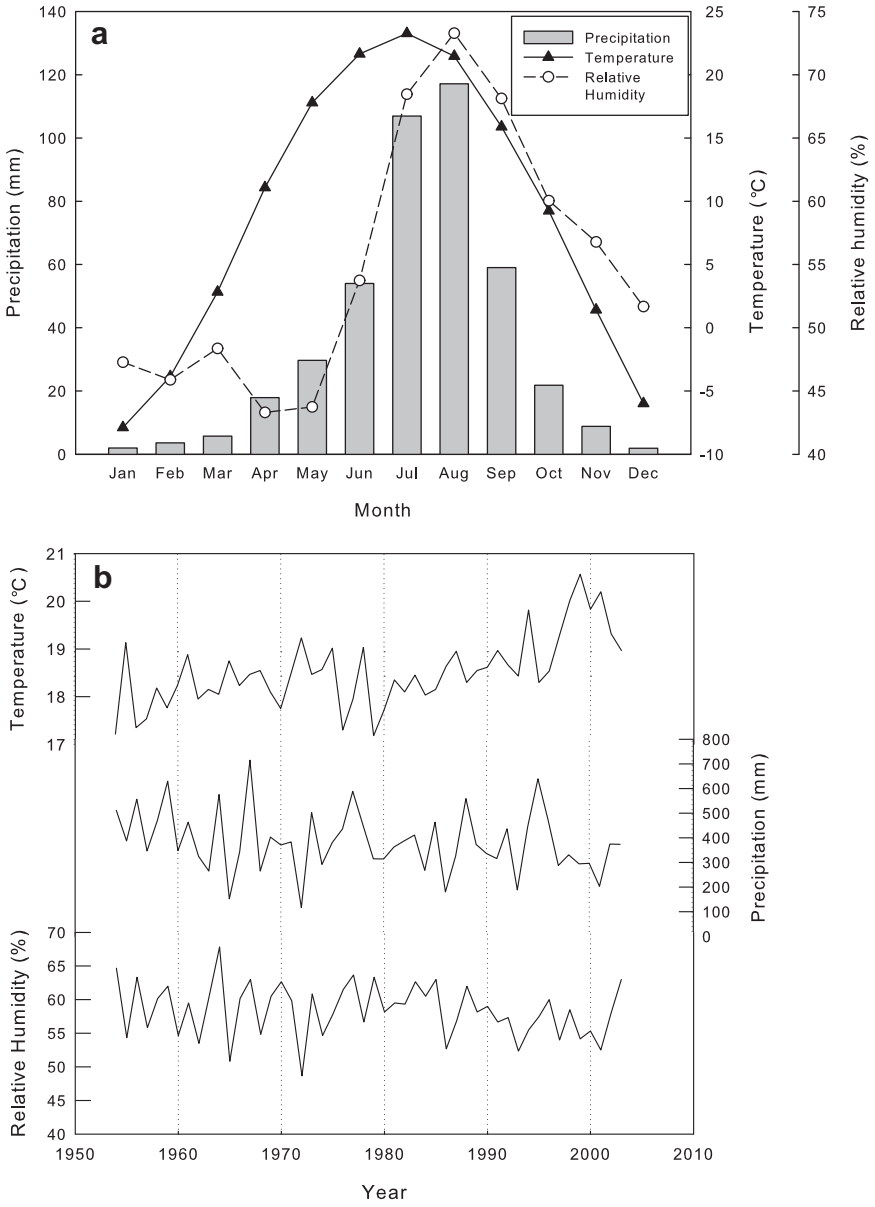

Fig. 2. Monthly mean precipitation, temperature and relative humidity (a) and inter-annual variations of total precipitation, mean temperature and relative humidity during the growing season of April–September (b) at the Yuanping station from 1954 to 2003.

The final standardized NW chronology extends from 1676 to 2003. The mean sensitivity indicates measurement of relative difference in widths between adjacent rings, which was 0.28 for NW chronology. One of the important requirements for time series is to determine the extent to which the mean value for each year is accurately captured. The chronology signal strength was evaluated using Subsample Signal Strength (SSS; Wigley et al., 1984). SSS is a measure of the quality of the tree-ring index curve, in which values close to 1 are achieved when trees reflect strong common growth variability at a site. To utilize the maximum length of the tree-ring chronology and ensure the accuracy of the reconstruction, the effective length of the chronology covered the period in which the SSS was at least 0.75. This threshold corresponds to the period 1779–2003, with a minimum sample depth of 10 cores (5 trees) in 1779. The statistical items of the NW chronology are listed in Table 1.

2.4. Climate data

For the climate response analysis of the tree-ring chronology, precipitation, relative humidity, maximum, minimum and mean temperatures were derived from the Yuanping meteorological station (38°45′N, 112°42′E; 836 m above sea level, records from 1954 to 2003). The data have been verified by Li et al. (2006, 2011b). In addition, precipitation, maximum, minimum and mean temperatures from the Climatic Research Unit TS3 (CRU TS3, http://badc.nerc.ac.uk/browse) dataset were also employed as a reference to investigate the climate responses. These climate parameters were used for climate-growth analysis over the common period 1954–2003. The CRU TS3 gridded temperature datasets, NCDC Sea Surface Temperature (SST) version 3b dataset (http://www.ncdc.noaa.gov/oa/climate/research/sst/ersstv3.php) and Hadley Centre Sea Level Pressure (Had SLP) version 2r dataset (http://hadobs.metoffice.com) were used to investigate the spatial correlation patterns, which were performed using the KNMI Climate Explorer (http://climexp.knmi.nl).

3. Results

3.1. Climate responses of the tree-ring width index

Pearson's coefficients of correlation were computed for climatic data and the tree-ring width chronology from the previous April to October of a given year. The results are shown in Fig. 3. As a whole, the tree-ring width index is positively correlated with precipitation and relative humidity, but negatively correlated with temperature during the growing season. Relative humidity is controlled by precipitation and temperature. For example, relative humidity has shared a similar trend with precipitation at the Yuanping meteorological station during the last 50 years ($r = 0.708$, $n = 50$, $p < 0.0001$). Therefore, only the precipitation/temperature–growth relationships are discussed. More specifically, summer months show a significant peak of correlation, indicating that the combination of precipitation and temperature during summer months

Table 1
Statistical items of the standardized chronology of NW.

Statistical items	NW
Mean sensitivity	0.28
Standard deviation	0.32
First-order autocorrelation	0.31
% Variance in 1st PC	41.13%
Mean correlation between all cores	0.363
Mean correlation between trees	0.343
Mean correlation within a tree	0.395
Subsample Signal Strength (SSS) ≥ 0.75 (trees)	1779 (5)

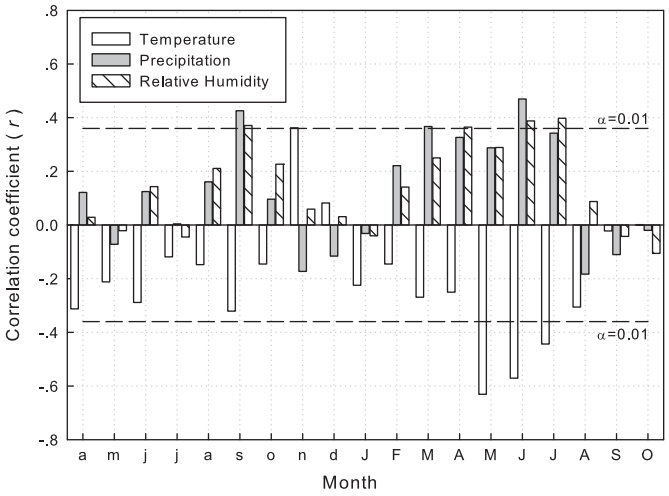

Fig. 3. The correlation between tree-ring width indices and monthly mean temperature, monthly total precipitation and monthly mean relative humidity form previous April to current October during 1954–2003. Meteorological data come from Yuanping. Horizontal dashed lines are the 99% confidence level.

controls the tree-ring growth in this region. By integrating different months, the highest correlation coefficient appears during the May–July temperature interval ($r = -0.672$, $n = 50$, $p < 0.001$) when using observed temperature from the Yuanping meteorological station, whereas the highest correlation coefficient is −0.548 ($n = 50$, $p < 0.001$) when using the CRU TS3 temperature data.

The significant negative correlation between the Chinese pine ring width and temperature in summer months has also been detected in northwestern China (Cai and Liu, 2007) and central China (Liu et al., 2001; Cai et al., 2008). As investigated by Xu (1990), Chinese pine mainly is distributed in regions in which the mean annual precipitation is approximately 500 mm. At the sampling site, the mean annual precipitation (428 mm) is less than 500 mm. The growth of trees is therefore very sensitive to soil water. As a result of shallow soil layers and the rocky environment of the sampling site, the soil has a limited ability to preserve water. Consequently, increasing summer temperature results in high evaporation rates of soil water and high transpiration rates inside leaves, leading to lower than normal growth.

3.2. Reconstruction of temperature variations

To reconstruct temperature variations, observed temperature recorded in the Yuanping meteorological station were regressed against the tree-ring width chronology for the period 1954–2003. Adjusting parameters of the regression model finally fixed the transfer function, which could explain 45.1% (44% after adjustment for loss of degrees of freedom) of the total variance for the actual May–July temperature during 1954–2003. In the model, $n = 50$, $r = 0.672$, $F = 39.454$, standard error = 0.641 and $p < 0.0001$. The comparison between observed and reconstructed May–July temperature is shown in Fig. 4a.

Temperature found in the reconstruction is approximately 0.8 °C lower than the temperature observed from 1997 to 2001, for which the actual temperature increased rapidly and reached the highest levels observed during the last 50 years. Yonenobu and Eckstein (2006) reported that tree-ring width in central Japan also did not follow a warming trend, which most likely resulted from anthropogenic SO_2 emissions. Furthermore, D'Arrigo et al. (2008) reviewed recent temperature reconstructions based on tree-ring

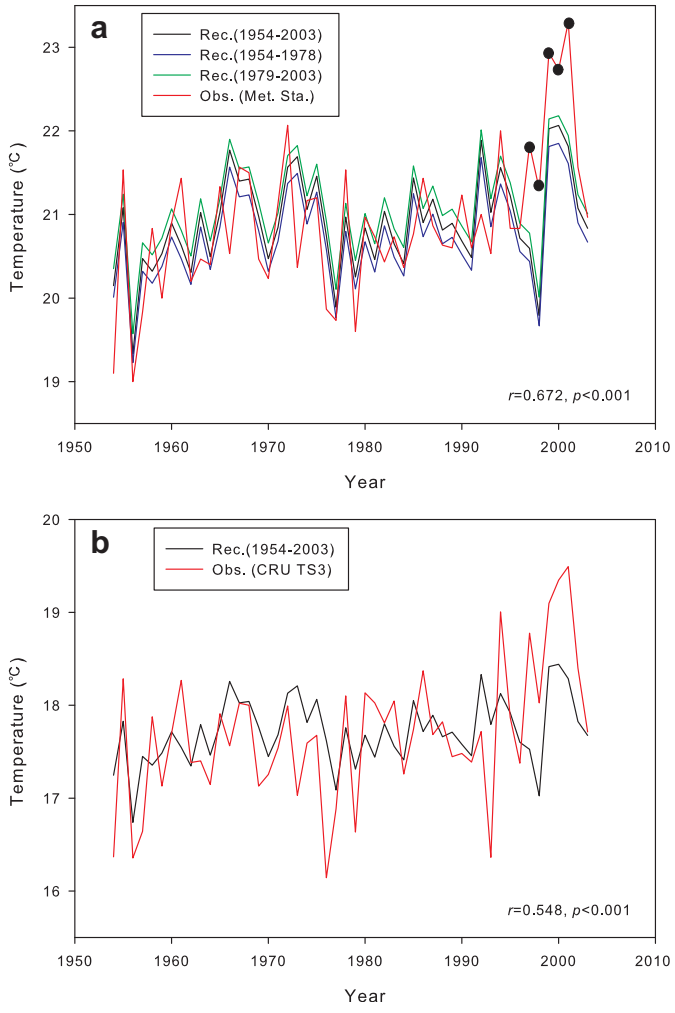

Fig. 4. Comparison between observed (Obs.) and reconstructed (Rec.) temperatures. Reconstructions based on different periods by ring-width indices and observed data from Yuanping meteorological station; (a) Reconstruction by ring-width indices and the CRU TS3 temperature data (b).

width and suggested that tree-ring width demonstrates the loss of temperature sensitivity in Northern Forests under rapid warming in the last few decades. This phenomenon may correlate with many factors such as temperature-induced drought stress, limitation of transfer function or uneven records of temperature used in transfer function, but the recognized mechanism has not identified until now. As shown in Fig. 2b, the temperature in the study area represents a rapid increase since the end of the 1980s. To understand the rapid warming trend better, three reconstruction models were established by linear regression between the ring-width index and the observed temperature during 1954–1978, 1979–2003 and 1954–2003, respectively. Then, the reconstructed results from those three models are compared with all period (1954–2003) of observation (Fig. 4a). Three reconstructions show the same variation and correlation ($r = 0.672$) as the observation during 1954–2003, revealing that the reconstruction based on 1979–2003 does not avoid the underestimated temperature of 1997–2001. The sampling site is located in a mountainous region and at a higher altitude (>2400 m above sea level), whereas the Yuanping meteorological station is located in a flat region and at a lower altitude (836 m above sea level). As a result of different actual temperatures at the sampling site and the Yuanping meteorological station, the average May–July temperature in the 38–39°N, 111–113°E region was derived from the CRU TS3 gridded dataset, to reconstruct the temperature based on the tree-ring width chronology (Fig. 4b), which did not eliminate the underestimated temperature found during 1997–2001.

High correlation between the tree-ring width indices and observed temperature during 1954–2003 was observed, Therefore, May–July temperature was reconstructed to emphasize the low-frequency variability and to investigate temperature responses to large-scale atmospheric circulations.

Fig. 5 shows the inter-annual to inter-decadal (11-year moving average data) variations of reconstructed May to July temperature for the NW. The period 1779–2003 represents an effective reconstruction, while the reconstruction in 1676–1778 remains a reference because of small sample sizes. The mean temperature is 20.96 °C in the reconstruction during 1779–2003. Several extended warm and cold periods (≥11 years) are detected. Warm periods occurred during approximately 1779–1792, 1827–1839, 1853–1865, 1898–1932, 1936–1948 and 1987–2003, while cold periods occurred during 1793–1807, 1814–1826, 1866–1888, 1949–1963 and 1976–1986.

4. Discussion

4.1. Spatial representative of the reconstructed temperature

To understand how large-area temperature variations could be represented by the reconstruction, spatial correlation analysis between reconstructed May–July temperature and the concurrent CRU TS3 temperature gridded dataset was carried out for the common period of 1901–2003. The results are plotted in Fig. 6, and indicate that the reconstruction is representative of a large-area, including three geographical regions. One region is the semi-arid North China Plain (NCP), which has been recognized as one of the most water-scarce regions in the world (Fu et al., 2009). Second is the semi-arid Loess Plateau (LP); the LP is the largest deposition zone of loess in the world (Liu et al., 2009c). Another region is the extremely arid Gobi Desert (Gobi), located at the boundary between China and the State of Mongolia. The Gobi is one of the largest deserts in Asia. Furthermore, the correlation field extends to the northwestern region of the State of Mongolia. For convenience,

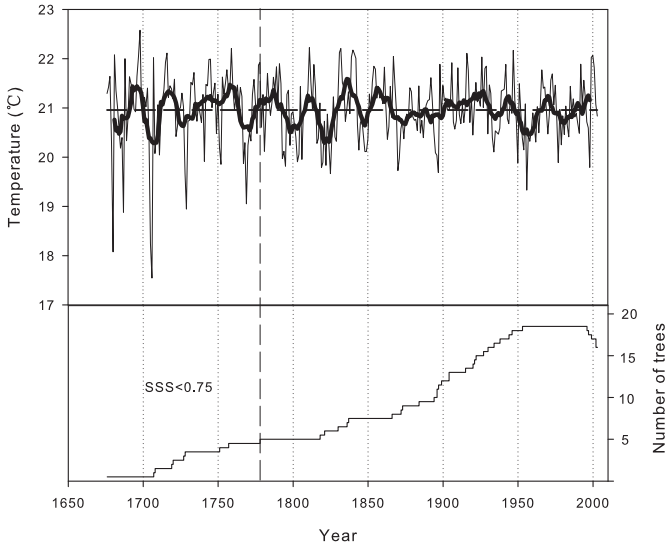

Fig. 5. Reconstructed May to July temperature variations (top). Thin and solid lines are annual and 11-year moving average data, respectively. Sample depth also is shown (bottom). Subsample Signal Strength (SSS) is higher than 0.75 since 1779.

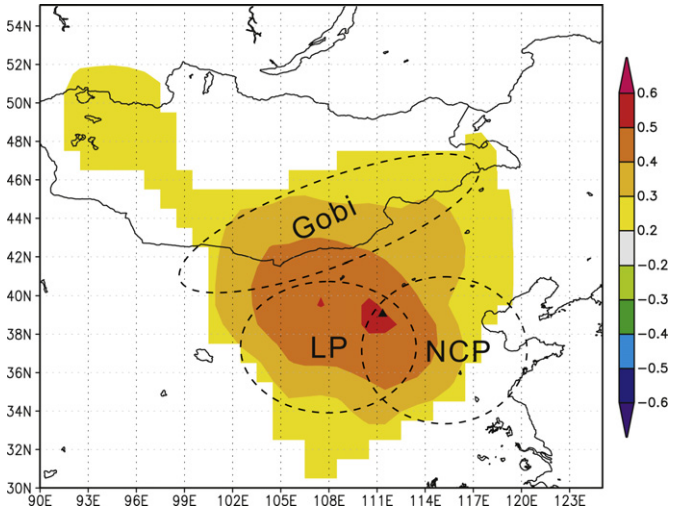

Fig. 6. Spatial correlation pattern between reconstructed May to July temperature and concurrent CRU TS3 temperature gridded dataset during 1901–2003. Dashed boxes showing schematic locations of the Gobi Desert (Gobi), the Loess Plateau (LP) and the North China Plain (NCP); solid triangle showing the sampling site.

this significant correlation region in Fig. 6 is referred to as North China.

To check the regional representatives of May–July temperature reconstruction during a longer period, other temperature reconstructions in North China were compared. Cai and Liu (2007) reconstructed January to August temperature in the Helan Mountains (38°27′N–39°30′N, 105°20′E–106°41′E) during 1776–1999. The correlation coefficients are 0.356 (n = 224) for the inter-annual scale, 0.283 (n = 214) for 11-year moving average data and 0.393 (n = 200) for 25-year moving average data (Table 2). In Fig. 7a and Fig. 7b, the reconstruction presents a synchronous variation with the reconstructed temperature for the Helan Mountains, although the distance between the sampling site and the Helan Mountains is very far (approximately 500 km; Fig. 1). In the last half century, the warming trend in the Helan Mountains is more obvious than that revealed by the reconstruction. This finding is attributed to the differences found in reconstructed seasons. The January–August temperature found in the Helan Mountains comprise some temperature signals in winter that have a more rapid warming trend than that of summer. For example, observed mean winter temperature variation in all of China is approximately 4 times than that of summer temperature during 1960–2006 (Piao et al., 2010). In addition, the summer warming trend in North China (<0.01 °C per year) is the lowest in comparison with other regions of China (Piao et al., 2010).

4.2. Link with EASM

The broad representation of regions in this reconstruction implies that large-scale atmospheric circulations influence temperatures in North China. In contrast to many studies of precipitation-atmospheric circulation relationships, there are very few investigations concerning the relationship between temperature and large-scale atmospheric circulation. Zhu et al. (2009) reconstructed February–April temperature by using tree-ring widths in Changbai Mountains, located in Northeast China. They suggested that the reconstruction might be a good indicator of the East Asian Winter Monsoon intensity. Liu et al. (2010) detected that the reconstructed May to June temperature of the Chifeng-Weichang region, Northeast China, using tree rings showed a significant (p < 0.0001) negative correlation with monsoon rainfall since 1884, suggesting that the dominant climate regime is either cool/wet or warm/dry.

The East Asian Monsoon exerts a large influence on climate in East Asia. In the summer, EASM brings large amounts of water vapor to North China, where summer precipitation accounts for approximately 60–80% of the total annual precipitation (Fig. 2a; Liu et al., 2010). The summer precipitation in this region thus can be seen to be an indicator of EASM intensity, namely, strong EASM results in heavy precipitation amounts. Han and Wang (2007) defined an EASM index as the normalized zonal wind shear (or difference) between 850 hPa and 200 hPa averaged over 20°N–40°N and 110°E–140°E in summer (June–August), which is significantly negatively correlated with the reconstructed May–July temperature (r = −0.262, p = 0.06, n = 50 at the inter-annual scale; r = −0.397, n = 40 at the decadal scale and r = −0.695, n = 26 at the multi-decadal scale). Because the EASM index is very short (50 years), it is not shown in Fig. 7. Instead, the reconstructed annual (previous August to current July) precipitation in Ningwu using tree-ring width (Fig. 7c; Li et al., 2006) was employed to investigate the relationship between the reconstructed May–July temperature in this study and monsoon precipitation during the common period of 1688–2003. Although there are some slight differences in trends that may be caused by differences in reconstructed seasons, the May–July temperature is generally synchronous and significantly negatively correlated with the annual precipitation (Fig. 7a and c). The correlation coefficients are −0.312 (n = 316) for the inter-annual scale, −0.266 (n = 306) for the decadal scale and −0.488 (n = 292) for multi-decadal scale (Table 2). The results suggest that the climate regime in North China is either cool/wet or warm/dry, and implies that the May–July temperature might be influenced by EASM.

In general, EASM anomalies are considered to be results of the atmospheric response to changes in thermal contrast between the East Asian domain and its adjacent oceans (Webster and Yang, 1992; Li and Yanai, 1996; Zhou et al., 2009a). To understand the mechanism of this relationship between temperature of North China and EASM, spatial correlation patterns between actual May to July temperature at the Yuanping meteorological station and Sea Surface Temperature (SST) datasets from NCDC (http://lwf.ncdc.noaa.gov/oa/climate/research/sst/sst.php) were investigated. In Fig. 8a, two fields are significantly positively correlated with the temperature of North China. One field is located in the Western North Pacific. When ocean warming was abnormal in this region, the enhanced Western Pacific Subtropical High (WPSH) extended westward (Zhou et al., 2009b). The other field is in the Philippine Sea. It was suggested that the increased SST of the Philippine Sea strengthened tropical convection, which also enhanced WPSH (Wu and Wang, 2002). The WPSH that was enhanced and extended westward also shifted southeasterly winds to northeasterly winds in North China, and EASM precipitation thus decreased below the normal level (Ninomiya and Kobayashi, 1999; Wu and Wang, 2002; Zhou et al., 2009c). Consequently, temperature in North China increased. In contrast, cooling SST of the oceans adjacent to East Asia induced a temperature decrease in North China.

Table 2
Correlation coefficients (r) between reconstructed May–July temperature and January to August temperature in the Helan Mountains (HL T18), previous August to current July precipitation in the Ningwu (NW P87), Summer APO (JJA APO) and annual PDO in inter-annual, decadal (11-year moving average data) and multi-decadal (25-year moving average data) time scales in the overlapping period.

	HL T18 (1796–1999)	NW P87 (1688–2003)	JJA APO (1676–1985)	Annual PDO (1676–1996)
Inter-annual	0.356	−0.312	−0.044	0.057
Decadal	0.283	−0.266	−0.249	0.244
Multi-decadal	0.393	−0.488	−0.684	0.660

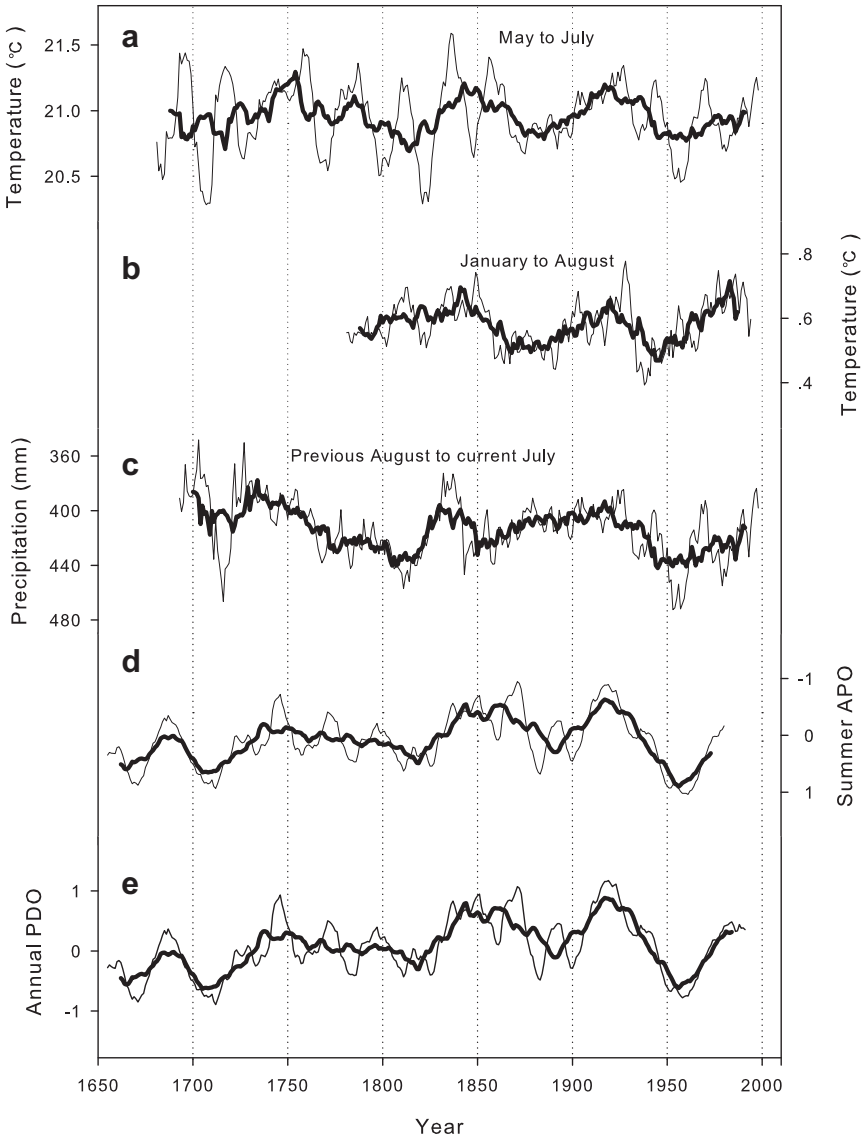

Fig. 7. Comparison between reconstructed May to July temperature in this study (a) and January to August temperature in the Helan Mts. (b), previous August to current July precipitation in Ningwu (c), summer APO (d) and annual PDO (e). Thin and solid curves are smoothed by 11- and 25-year moving average, respectively.

Moreover, the relationship between temperature in North China and EASM can be explained by investigating the spatial correlation between the actual May–July temperature and concurrent Sea Level Pressure (SLP) from the HadSLP2 dataset (http://hadobs.metoffice.com/hadslp2/). EASM strength, which is defined by the summation of SLP gradients between the land and sea, is the most widely used index in EASM studies (Guo, 1983; Wang and LI, 2007; Zhou et al., 2009b). Fig. 8b shows a significantly negative correlation field in the Western Pacific between the temperature and SLP. Depressed SLP in this region implies that EASM becomes weaker than normal, which results in low precipitation amounts and high temperature in North China (Wang et al., 2008).

4.3. Link with APO

The Asian-Pacific Oscillation (APO), a zonal teleconnection pattern over the extratropical Asian-Pacific region, has been identified (Zhao et al., 2007). APO index was defined as the summer upper-tropospheric (500–200 hPa) temperature difference between the Asian domain (15°N–50°N, 60°E–120°E) and the North Pacific (15°N–50°N, 180°W–120°W). It showed a decadal variation. Several studies have indicated that APO has a significant impact on climate in China (Zhao et al., 2007, 2008; Zhou et al., 2009a; Zhou and Zhao, 2010). Zhou et al. (2009a) have reconstructed summer (June–August) APO index over the past millennium, which is shown in Fig. 7d. The correlation between reconstructed May–July temperature and summer APO index at an inter-annual scale is not significant ($r = -0.044$, $n = 310$). At decal and multi-decadal time scales, however, the correlation coefficients increase greatly to −0.249 ($n = 300$) and −0.684 ($n = 286$), respectively (Table 2); this is reasonable because APO is closely correlated with PDO characterized by decadal to multi-decadal cycles (Mantua et al., 1997; Zhao et al., 2007; Zhou and Zhao, 2010). The physical mechanism for such a relationship (reconstructed temperature-APO) could be explained as follows. A positive phase of APO, with characteristics of a positive anomaly in upper-tropospheric temperatures over Asia and a negative anomaly over the North Pacific, results in an anomaly of the low-level southerlies prevailing at the mid-latitudes of East China during

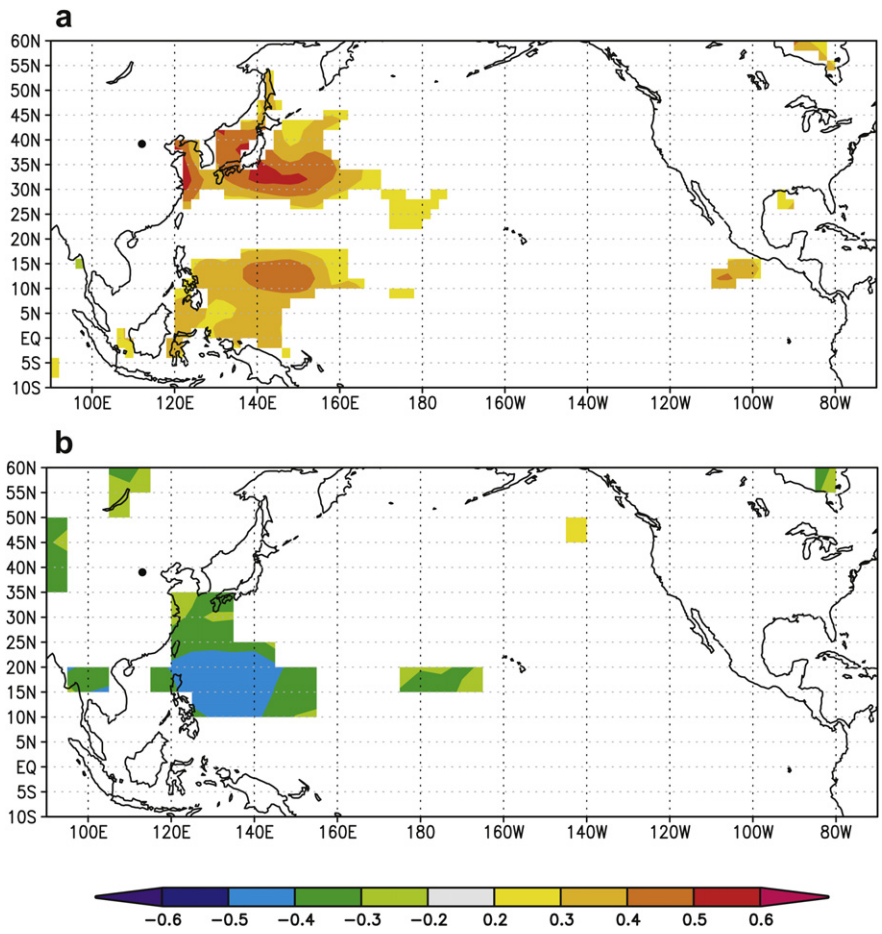

Fig. 8. Spatial correlation patterns between observed May to July temperature in study area and concurrent SST dataset from NCDC (a) and SLP from HadSLP2 dataset (b) during 1954–2003.

the summer. This condition is favorable for the transport northward of water vapor, leading to increased precipitation in North China (Zhao et al., 2007; Zhou and Zhao, 2010). The temperature may become cool because of the climate regime of either cool/wet or warm/dry in North China, and *vice versa*.

4.4. Link with PDO

Mantua et al. (1997) have detected a robust recurring pattern of ocean–atmosphere climate variability with multi-decadal cycles centered over the mid-latitude North Pacific basin (the Pacific Decadal Oscillation or PDO), and many studies found the influence of observed PDO on hydroclimate parameters (precipitation or PDSI) in Asia (D'Arrigo and Wilson, 2006; Ma, 2007; Sano et al., 2009; Fang et al., 2010). Little is known, however, about the impact of PDO on temperatures in Asia.

It has been suggested that there were three regime shifts of PDO in the 1920s, 1940s and 1970s (Mantua et al., 1997; Hare and Mantua, 2000) and one climate regime shift in 1750s by reconstruction (Biondi et al., 2001). The climate regime shifts above correspond with four temperature shifts in the reconstruction (Fig. 7a). Furthermore, a comparison of the reconstructed May–July temperature in this study and reconstructed PDO by MacDonald and Case (2005) suggests that there is a close link in the past three centuries (Fig. 7e). The correlation at the inter-annual scale is very low ($r = 0.057$, $n = 321$). The correlation is significantly high ($r = 0.660$, $n = 297$) at the multi-decadal scale by a using 25-year moving average because of a 20–30 year cycle of PDO. Liu et al. (2009b) also reported a significant correlation between PDO and the reconstructed May to June temperature in Weichang, Northeast China, during 1884–2002.

PDO is defined as warm or cool surface waters in the North Pacific (north of 20°N). During a warm phase, the west Pacific becomes cool and part of the eastern ocean warms; during a cool phase, the opposite pattern occurs. Because climate in the North China is mainly controlled by the East Asian Monsoon influenced by a land–sea thermal contrast, PDO therefore must have some impact on climate in North China. Ma (2007) summarized that a warm phase of PDO in the last 50 years corresponded with high temperature in North China. The physical mechanism of this link is still not well understood (Ma, 2007).

5. Conclusions

A tree-ring width chronology from 1686 to 2003 was developed using 37 tree-ring cores in Ningwu, Shanxi Province, China. The chronology is most reliable after 1779, for the period in which SSS equals 0.75. Because of significantly negative correlation ($r = -0.672$, $n = 50$, $p < 0.001$) between the chronology and local May–July temperature, this chronology was employed to reconstruct the temperature variability from May to July. The spatial correlation pattern indicates that the reconstruction is representative of large-area temperature variability in some regions of China and the State of Mongolia, including the Gobi Desert, the Loess Plateau and the North China Plain. The reconstructed temperature is in agreement with reconstruction of January–August

temperature in the Helan Mountains, which are approximately 500 km away from Ningwu.

The reconstruction of temperature is significantly negative correlated with monsoon rainfall at inter-annual, decadal and multi-decadal time scales, suggesting the dominant climate regime is either cool/wet or warm/dry in North China, which is the same as the climate regime in Northeast China (Liu et al., 2010).

In addition, a significantly negative (positive) correlation between the reconstruction of temperature in North China and APO (PDO) at both decadal and multi-decal scales in the past three centuries suggests the influences of large-scale atmospheric circulations on regional temperature in North China.

Acknowledgements

We are very grateful to Prof. Xiuji Zhou for providing the reconstructed APO data, and Shaohua Song, Jungang Dong and Lei Wang for the help in the fieldwork. This study was financially supported by the National Natural Science Foundation of China (No. 40890050), KZZD-EW-04, the Hundred Talents Program of the Chinese Academy of Sciences and the State Key Laboratory of Loess and Quaternary Geology (No. SKLLQG1110) .This is Sino-Swedish Tree-ring Research Center (SISTRR) contribution (013).

References

Biondi, F., Gershunov, A., Cayan, D.R., 2001. North Pacific decadal climate variability since 1661. Journal of Climate 14, 5–10.

Buckley, B.M., Palakit, K., Duangsathaporn, K., Sanguantham, P., Prasomsin, P., 2007. Decadal scale droughts over northwestern Thailand over the past 448 years: links to the tropical Pacific and Indian Ocean sectors. Climate Dynamics 29, 63–71.

Cai, Q., Liu, Y., 2007. January to August temperature variability since 1776 inferred from tree-ring width of *Pinus tabulaeformis* in Helan Mountain. Journal of Geographical Sciences 17 (3), 293–303.

Cai, Q.F., Liu, Y., Song, H.M., Sun, J.Y., 2008. Tree-ring-based reconstruction of the April to September mean temperature since 1826 AD for north-central Shaanxi Province, China. Science in China Series D: Earth Sciences 51 (8), 1099–1106.

Cook, E.R., Kairiukstis, L., 1990. Methods of Dendrochronology. Kluwer Dordrecht, The Netherlands.

Cook, E.R., Anchukaitis, K.J., Buckley, B.M., D'Arrigo, R.D., Jacoby, G.C., Wright, W.E., 2010. Asian monsoon failure and megadrought during the last millennium. Science 328 (5977), 486.

D'Arrigo, R., Wilson, R., 2006. On the Asian expression of the PDO. International Journal of Climatology 26 (12), 1607–1617.

D'Arrigo, R., Wilson, R., Liepert, B., Cherubini, P., 2008. On the divergence problem in northern forests: a review of the tree-ring evidence and possible causes. Global and Planetary Change 60 (3–4), 289–305.

Dillon, M.E., Wang, G., Huey, R.B., 2010. Global metabolic impacts of recent climate warming. Nature 467 (7316), 704–706.

Ding, Q., Wang, B., 2007. Intraseasonal teleconnection between the summer Eurasian Wave Train and the Indian monsoon. Journal of Climate 20, 3751–3767.

Fang, K., Gou, X., Chen, F., Li, J., D'Arrigo, R., Cook, E., Yang, T., Davi, N., 2010. Reconstructed droughts for the southeastern Tibetan Plateau over the past 568 years and its linkages to the Pacific and Atlantic Ocean climate variability. Climate Dynamics 35 (4), 577–585.

Fu, G., Charles, S.P., Yu, J., Liu, C., 2009. Decadal climatic variability, trends, and future scenarios for the North China Plain. Journal of Climate 22 (8), 2111–2123.

Garfin, G.M., Hughes, M.K., Yu, L., Burns, J.M., Touchan, R., Leavitt, S.W., Zhisheng, A., 2005. Exploratory temperature and precipitation reconstructions from the Qinling Mountains, north-central China. Tree-Ring Research 61 (2), 59–72.

Guo, Qi-Yun, 1983. The summer monsoon intensity index in East Asia and its variation. Acta Geographica Sinica 38, 207–217 (in Chinese).

Han, J.P., Wang, H.J., 2007. Features of interdecadal changes of the East Asian Summer Monsoon and similarity and discrepancy in ERA-40 and NCEP/NCAR reanalysis. Chinese Journal of Geophysics 50 (6), 1666–1676 (in Chinese with English abstract).

Hare, S.R., Mantua, N.J., 2000. Empirical evidence for North Pacific regime shifts in 1977 and 1989. Progress in Oceanography 47 (2–4), 103–145.

Holmes, R.L., 1983. Computer-assisted quality control in tree-ring dating and measurement. Tree-ring Bulletin 43 (1), 69–78.

Hughes, M.K., Xiangding, W., Xuemei, S., Garfin, G.M., 1994. A preliminary reconstruction of rainfall in north-central China since AD 1600 from tree-ring density and width. Quaternary Research 42 (1), 88–99.

Lau, K.M., Li, M.T., 1984. The monsoon of East Asia and its global associations: a survey. Bulletin of the American Meteorological Society 65, 114–125.

Li, C., Yanai, M., 1996. The onset and interannual variability of the Asian summer monsoon in relation to land–sea interactive thermal contrast. Journal of Climate 9, 358–375.

Li, Q., Liu, Y., Cai, Q.F., Sun, J.Y., Yi, L., Song, H.M., Wang, L., 2006. Reconstruction of annual precipitation since 1686 A.D. from Ningwu region, Shanxi Province. Quaternary Sciences 26, 999–1006 (in Chinese with English abstract).

Li, Q., Nakatsuka, T., Kawamura, K., Liu, Y., Song, H., 2011a. Hydroclimate variability in the north China Plain and its link with El Niño–southern oscillation since 1784 AD: insights from tree-ring cellulose $\delta^{18}O$. Journal of Geophysical Research 116 (D22), D22106.

Li, Q., Nakatsuka, T., Kawamura, K., Liu, Y., Song, H., 2011b. Regional hydroclimate and precipitation $\delta^{18}O$ revealed in tree-ring cellulose $\delta^{18}O$ from different tree species in semi-arid Northern China. Chemical Geology 282, 19–28.

Liu, Y., Ma, L., Hughes, M., Garfin-Woll, G., Cai, Q., An, Z., Leavitt, S., 2001. Seasonal temperature reconstruction from central China based on tree ring data. Palaeobotanist 50, 89–94.

Liu, Y., Ma, L., Leavitt, S.W., Cai, Q., Liu, W., 2004. A preliminary seasonal precipitation reconstruction from tree-ring stable carbon isotopes at Mt. Helan, China, since AD 1804. Global and Planetary Change 41, 229–239.

Liu, Y., Bao, G., Song, H., Cai, Q., Sun, J., 2009a. Precipitation reconstruction from Hailar pine (*Pinus sylvestris* var. *mongolica*) tree rings in the Hailar region, Inner Mongolia, China back to 1865 AD. Palaeogeography, Palaeoclimatology, Palaeoecology 282, 81–87.

Liu, Y., Tian, H., Song, H., Liang, J., Cai, Q., Sun, J., 2009b. Tree ring based reconstruction of the May–June mean temperature since A.D. 1884 in Weichang, Hebei Province. China Quaternary Sciences 29, 1–8 (in Chinese with English abstract).

Liu, Y., Linderholm, H.W., Song, H., Cai, Q., Tian, Q., Sun, J., Chen, D., Simelton, E., Seftigen, K., Tian, H., 2009c. Temperature variations recorded in *Pinus tabulaeformis* tree rings from the southern and northern slopes of the central Qinling Mountains, central China. Boreas 38, 285–291.

Liu, Y., Tian, H., Song, H., Liang, J., 2010. Tree ring precipitation reconstruction in the Chifeng-Weichang region, China, and East Asian Summer Monsoon variation since AD 1777. Journal of Geophysical Research 115, D06103.

Ma, Z.G., 2007. The interdecadal trend and shift of dry/wet over the central part of North China and their relationship to the Pacific Decadal Oscillation (PDO). Chinese Science Bulletin 52, 2130–2139.

MacDonald, G.M., Case, R.A., 2005. Variations in the Pacific Decadal Oscillation over the past millennium. Geophysical Research Letters 32 (8), L08703. doi:10.1029/2005GL022478.

Mantua, N.J., Hare, S.R., Zhang, Y., Wallace, J.M., Francis, R.C., 1997. A Pacific interdecadal climate oscillation with impacts on salmon production. Bulletin of the American Meteorological Society 78, 1069–1080.

Ninomiya, K., Kobayashi, C., 1999. Precipitation and moisture balance of the Asian summer monsoon in 1991: part II: moisture transport and moisture balance. Journal of the Meteorological Society of Japan 77, 77–99.

Piao, S., Ciais, P., Huang, Y., Shen, Z., Peng, S., Li, J., Zhou, L., Liu, H., Ma, Y., Ding, Y., 2010. The impacts of climate change on water resources and agriculture in China. Nature 467, 43–51.

Sano, M., Buckley, B.M., Sweda, T., 2009. Tree-ring based hydroclimate reconstruction over northern Vietnam from *Fokienia hodginsii*: eighteenth century mega-drought and tropical Pacific influence. Climate Dynamics 33, 331–340.

Shao, X., Huang, L., Hongbin, L., Eryuan, L., Xiuqi, F., Lili, W., 2005. Reconstruction of precipitation variation from tree rings in recent 1000 years in Delingha, Qinghai. Science in China Series D: Earth Sciences 48, 939–949.

Sheppard, P., Tarasov, P., Graumlich, L., Heussner, K.U., Wagner, M., Sterle, H., Thompson, L., 2004. Annual precipitation since 515 BC reconstructed from living and fossil juniper growth of northeastern Qinghai Province, China. Climate Dynamics 23, 869–881.

Stokes, M., Smiley, T.L., 1968. An Introduction to Tree Ring Dating, edited. University of Chicago Press, Chicago, IL.

Wang, B., 2001. Interannual variability of the Asian summer monsoon: contrasts between the Indian and the Western north Pacific–East Asian Monsoons. Journal of Climate 14, 4073–4090.

Wang, S., LI, W., 2007. Climate of China. China Meteorological Press, Beijing, 428 pp.

Wang, J., Chen, F., Jin, L., Guo, J., 2008. Relationships between climatic anomaly in arid region of central-east Asia and sea level pressure anomaly in the last 100 years. Plateau Meteorology 27 (1), 84–95 (in Chinese with English abstract).

Webster, P.J., Yang, S., 1992. Monsoon and ENSO: selectively interactive systems. Quarterly Journal of the Royal Meteorological Society 118, 877–926.

Wigley, T., Briffa, K., Jones, P., 1984. On the average value of correlated time series, with applications in dendroclimatology and hydrometeorology. Journal of Climate and Applied Meteorology 23, 201–213.

Wu, R., Wang, B., 2002. A contrast of the East Asian Summer Monsoon-ENSO relationship between 1962–77 and 1978–93. Journal of Climate 15, 3266–3279.

Xu, H., 1990. Chinese Pine. Chinese Forestry Press, Beijing.

Yonenobu, H., Eckstein, D., 2006. Reconstruction of early spring temperature for central Japan from the tree-ring widths of Hinoki cypress and its verification by other proxy records. Geophysical Research Letters 33 (10), L10701. doi:10.1029/2006GL026170.

Zhao, P., Zhu, Y., Zhang, R., 2007. An Asian-Pacific teleconnection in summer tropospheric temperature and associated Asian climate variability. Climate Dynamics 29, 293–303.

Zhao, P., Chen, J., Xiao, D., Nan, S., Zou, Y., Zhou, B., 2008. Summer Asian-Pacific oscillation and its relationship with atmospheric circulation and monsoon rainfall. Acta Meteorologica Sinica 66, 716–729 (in Chinese with English abstract).

Zhou, B., Zhao, P., 2010. Influence of the Asian-Pacific Oscillation on the spring precipitation over central eastern China. Advances in Atmospheric Science 27, 575–582.
Zhou, X.J., Zhao, P., Liu, G., 2009a. Asian-Pacific Oscillation index and variation of East Asian Summer Monsoon over the past millennium. Chinese Science Bulletin 54, 3768–3771.
Zhou, T., Gong, D., Li, J., Li, B., 2009b. Detecting and understanding the multi-decadal variability of the East Asian Summer Monsoon recent progress and state of affairs. Meteorologische Zeitschrift 18 (4), 455–467.
Zhou, T., Yu, R., Zhang, J., Drange, H., Cassou, C., Deser, C., Hodson, D.L.R., Sanchez-Gomez, E., Li, J., Keenlyside, N., 2009c. Why the Western Pacific subtropical high has extended westward since the late 1970s. Journal of Climate 22, 2199–2215.
Zhou, M., Tian, F., Lall, U., Hu, H., 2011. Insights from a joint analysis of Indian and Chinese monsoon rainfall data. Hydrology and Earth System Sciences Discussions 8, 3167–3187.
Zhu, H., Fang, X., Shao, X., Yin, Z., 2009. Tree ring-based February–April temperature reconstruction for Changbai Mountain in Northeast China and its implication for East Asian Winter Monsoon. Climate of the Past 5, 661–666.